

Soft Matter

Accepted Manuscript



This is an *Accepted Manuscript*, which has been through the Royal Society of Chemistry peer review process and has been accepted for publication.

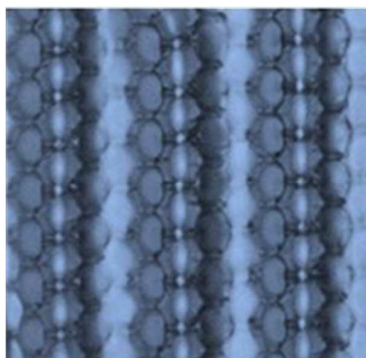
Accepted Manuscripts are published online shortly after acceptance, before technical editing, formatting and proof reading. Using this free service, authors can make their results available to the community, in citable form, before we publish the edited article. We will replace this *Accepted Manuscript* with the edited and formatted *Advance Article* as soon as it is available.

You can find more information about *Accepted Manuscripts* in the [Information for Authors](#).

Please note that technical editing may introduce minor changes to the text and/or graphics, which may alter content. The journal's standard [Terms & Conditions](#) and the [Ethical guidelines](#) still apply. In no event shall the Royal Society of Chemistry be held responsible for any errors or omissions in this *Accepted Manuscript* or any consequences arising from the use of any information it contains.

Graphical Abstract

A new structural design for wrinkling to improve mechanical durability by exploiting a porous polymer film embedded at the surface of an elastomer is proposed. The embedded thin porous film acts as a hard layer, which buckles into wrinkles, and the interpenetrated structure effectively suppresses fatal failures such as delamination and cracking.



COMMUNICATION

Reinforced shape-tunable microwrinkles formed on a porous-film-embedded elastomer surface

Cite this: DOI: 10.1039/x0xx00000x

T. Ohzono,^{*a} Y. Hirai,^b K. Suzuki,^a M. Shimomura^b and N. Uchida^cReceived 00th January 2012,
Accepted 00th January 2012

DOI: 10.1039/x0xx00000x

www.rsc.org/

A new structural design is proposed for wrinkling to improve mechanical durability by exploiting a porous polymer film embedded at the surface of an elastomer, which acts as a hard layer, buckles into wrinkles and effectively suppresses fatal failures such as delamination and cracking.

Wrinkling of thin elastic films supported by deformable substrates¹ has been exploited in a diverse variety of applications such as micropatterning², tunable optics,^{3–5} colloid patterning,^{6–9} cell proliferation,¹⁰ metrology of thin materials,^{11–13} electronics,¹⁴ energy harvesting,¹⁵ tunable wetting,¹⁶ microfluidics,¹⁷ gas sensing¹⁸ and adhesion.¹⁹ One of the characteristic features of wrinkled surfaces is their shape-tunability in response to changes in the applied strain.^{20,21} This property may be significantly advantageous for the above-mentioned applications, as it would impart reversibility and tunability of the surface functions. However, the shape-tunability of typical wrinkles with a sinusoidal waveform, which are formed on a flat film simply adhered to a soft substrate, e.g., a

polydimethylsiloxane (PDMS) elastomer, or on a plasma-treated substrate (PDMS) surface under compressive strain, is usually limited by their mechanical fragility as follows. Generally, the top films (with Young's modulus typically over hundreds of megapascals) supported by a substrate cannot elastically accommodate a high strain, s , (e.g., 0.1–0.2), resulting in crack formation⁶ or plastic deformation (yielding). Moreover, the adhesion between films and the substrate often cannot withstand the internal stress associated with the formation of wrinkles, leading to partial delamination known as buckling delamination.²² Such wrinkles are easily perturbed or destroyed by the application of large strains, repeated straining cycles, or mechanical rubbing. Consequently, it is difficult to directly utilize such wrinkles for applications that require a certain level of mechanical durability, e.g., tribological interfaces or switching elements with repeated structural changes. Thus, the use of wrinkles has been limited to an easy-to-make template for micropatterns. Thus, for use in tribological tests, patterns imprinted into other mechanically robust materials are employed,²³ however, these materials do not possess the unique shape-tunability of

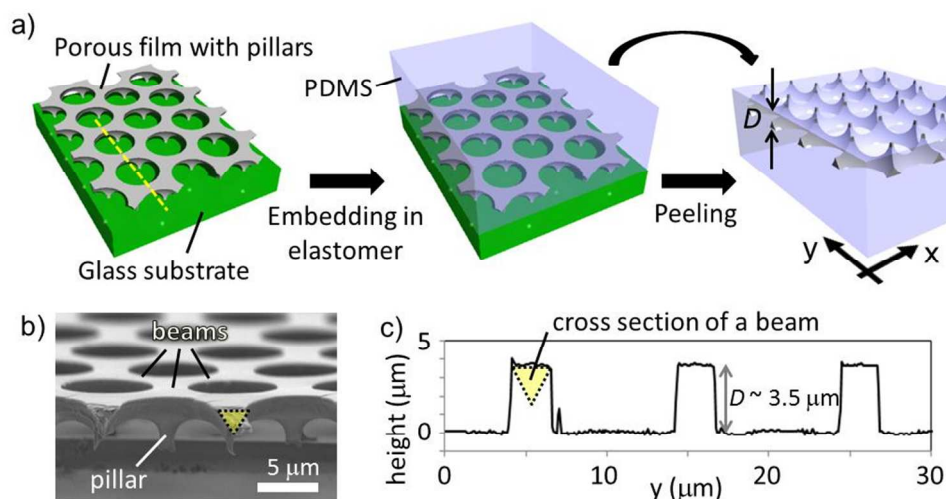


Fig. 1. Preparation of the porous-film-embedded elastomer. (a) Embedding procedure. (b) An SEM image of the porous film with pillars on a glass substrate. (c) The height profile of the pre-embedding porous film measured along the yellow-broken line indicated in (a), as obtained using a laser scanning optical microscope. The cross sections of a beam are indicated by yellow triangles.

COMMUNICATION

wrinkles,^{20,21} and this limits the controllability of tribological properties.

In this paper, we propose a new design for a layered wrinkling structure with improved mechanical durability achieved by exploiting a porous polymer film embedded at an elastomer surface. The porous film, which possesses two-dimensional hexagonal symmetry and pillars (or spikes)²⁴ protruding in an out-of-plane direction, acts as a hard layer that buckles into wrinkles. We discuss a qualitative feature, namely, strain-induced surface wrinkling, of the sample in which the porous film is embedded; the discussion is aided with a simple simulation result. Further, we demonstrate that owing to the gauche framework of a porous film embedded in a soft elastic substrate, the interpenetrated structure is beneficial for reducing delamination and cracking of the layer on which wrinkle formation occurs.

The porous polymer film to be embedded in a PDMS substrate is processed from a self-organized honeycomb-like porous film (Fig. S1)^{24,25} and prepared on a glass substrate [Fig. 1a and see Supplementary Information (SI) 1 for experimental details]. A precured PDMS fluid is poured on the porous film and the film-embedded PDMS is peeled off from the glass substrate after curing. Although some pillar apexes are exposed to air at the surface (Fig. 2a), most parts of the porous film are buried within PDMS. Thus, the top surface of the sample is almost flat except the pillar locations, which show a slight depression of 50–200 nm (Fig. 2c and 2e). When a uniaxial strain (s) is applied, the surface buckles into

wrinkles, showing some characteristic stripe patterns with different regularities in a manner that depends on the misfit angle ϕ [which is defined as the angle between the strain direction and x -axis attached to the hexagonal lattice (Fig. S2)]. Irrespective of ϕ , the wrinkle wavelength (λ) is typically $\lambda \sim 34 \pm 7 \mu\text{m}$ at $s = 0.1$, suggesting that the surface layer with the porous film having a thickness D acts as a hard film with rigidity roughly close to isotropic bending rigidity on a macroscopic length scale. Thus, we focus on the stripe pattern with $\phi \sim 0$ (Figs. 2b, 2c, 2d, and S2), which shows a particular regularity (Fig. 2g), for simplicity of the following discussion. In this case, the wavelength shows a simple geometrical relationship given by $\lambda = n(3^{1/2}/2)[A(1-s)]$, where n is an integer and is typically equal to 4, and A ($\sim 11 \mu\text{m}$) is the periodicity of holes in the porous film. It should be noted that wrinkle crests and grooves appear at the middle of beams of the porous film, which are assumed to be the parts with the least bending rigidity. The wrinkle depth, $2A$, increases with s in an inverse-quadratic manner (Fig. 3a), which is typical of a wrinkling system.¹

Assuming that the present wrinkling phenomenon can be qualitatively explained by the conventional model for the wrinkling of a flat surface layer supported by a soft substrate,¹ we can estimate the bending rigidity of the “effective hard layer to wrinkling” in the present system as follows. According to the conventional model, the wrinkle wavelength at the minimum buckling strain is expressed as $\lambda_0 = 2\pi H [(1 + \nu_s)/6(1 - \nu_r^2)]^{1/3} [E_r/E_s]^{1/3}$, where H is the imaginary thickness of the effective hard layer,²⁶ ν and E are Poisson’s ratio

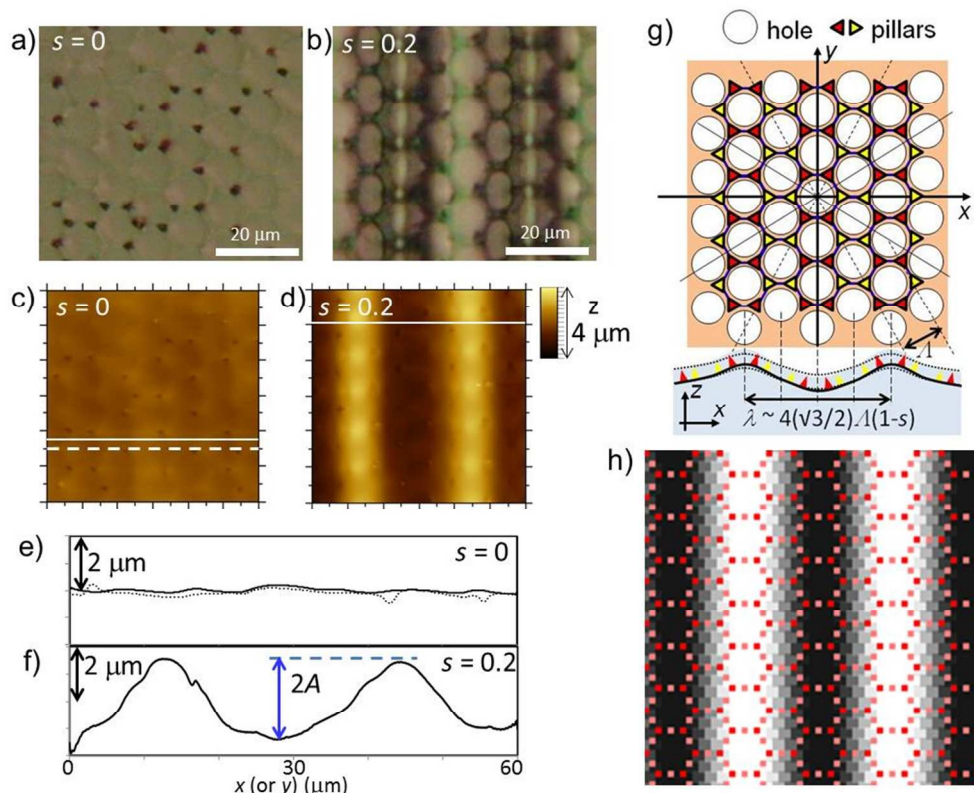


Fig. 2. Wrinkling of the porous-film-embedded elastomer surface with $\phi = 0$ (see Fig. S2). (a) and (b) Optical microscopy images. (a) is the image taken before strain application. (c) and (d) AFM images ($60^2 \mu\text{m}^2$), and (e) and (f) the corresponding AFM profiles along the lines indicated in (c) and (d), respectively. (c) is the image taken after 100 compression–decompression cycles, showing neither clear damage nor undulations. (g) A schematic for the wrinkled state with $\phi = 0$ and the hexagonal regularity of the embedded porous film. (h) A profile obtained from a simple model simulation on a triangular lattice. At the red and pink points, which correspond to pillars and beams, respectively, the membrane has 10 and 5 times larger effective thickness than at the other points (see SI 3).

and Young's modulus, respectively, and indexes "s" and "f" represent the PDMS substrate and effective surface layer, respectively. The effective bending rigidity can be calculated using the relation $\kappa = \lambda_0^3 E_s / [2(2\pi)^3(1 + \nu_s)] = E_f H^3 / [12(1 - \nu_f^2)]$. Putting the actual values $\lambda_0 \sim 4(3^{1/2}/2)A \sim 38 \mu\text{m}$, $E_s \sim 1.3 \text{ MPa}$,^{4,13} and $\nu_s \sim 0.5$, in the former relation, we find the value of κ to be $\sim 74 \times 10^{-12} \text{ N m}^2$.

Further, we can also estimate the bending rigidity (κ^*) of a virtual "plane" polymer film that has an identical mass per unit area to that of the present porous film. Assuming the volume fraction (α) of the porous film within the top layer with the thickness $D \sim 3.5 \mu\text{m}$ (Fig. 1a) to be in the range $\alpha \sim 0.1\text{--}0.2$ (estimated as the volume fraction of the remaining part of the two-dimensionally closed-packed spheres in a layer with thickness close to the sphere diameter), the imaginary thickness of the "plane" polymer film is given by $d = \alpha D = 0.35\text{--}0.7 \mu\text{m}$. Using the relationship $\kappa^* = E_f d^3 / [12(1 - \nu_f^2)]$ with $E_f \sim 1.2 \text{ GPa}$ and $\nu_f \sim 0.35$ for polystyrene²⁷ used in the present study, which accounts for 91% of the polymer mixture, we obtain $\kappa^* = 4.9 \times 10^{-12}\text{--}39.1 \times 10^{-12} \text{ N m}^2$, which is less than κ . This result suggests that the effective bending rigidity of the surface layer is increased by employing the porous film. The result can be mainly attributed to the effect of the geometrical factor on bending rigidity; this effect is similar to that observed in corrugated plates that show higher bending rigidity in a specific direction as compared to those in other directions (SI 2).

The present characteristic wrinkle wavelength (λ) is only 3–4 times that of the periodicity of the porous structure (A) with hexagonal symmetry. It is already known that in such a case, the local wrinkle structure couples to the imprinted structural and/or modulus patterns.²⁸ In the present system, the top surface is almost flat and the modulus distribution pattern exists because of the embedded regular porous film. Thus, to confirm that the observed wrinkle structure is influenced by the modulus pattern, we simply model the present system as a flat film that has a two-dimensional modulus distribution corresponding to a hexagonal lattice and is supported by a soft substrate (SI 1 and SI 3). As a result, a wrinkle structure (Fig. 2h) similar to that observed (Fig. 2b and 2d) is obtained, in which wrinkle crests and grooves appear at the part corresponding to the beams parallel to the compression direction (x axis). This qualitatively indicates that the present local coupling of wrinkles to the imprinted pattern is due to the two-dimensional modulus pattern in the effective hard surface layer.

Next, we demonstrate the mechanical durability of the present shape-tunable microwrinkles. Even after repeated compression–decompression cycles (~ 100) between $s = 0$ and 0.2 , no clear difference is observed in the dependence of the wrinkle depth ($2A$) on strain (Fig. 3a). Moreover, the top surface shows neither cracks nor delamination. In contrast, PDMS simply coated with a PSt film (PSt/PDMS, see SI 1) easily starts showing delaminated crests and cracks perpendicular to the groove direction at s values around $0.1\text{--}0.15$ (Fig. 3b). Although the present porous film appears to be partially delaminated from the PDMS matrix (Fig. 3a, inset) and to be plastically deformed, these cause no critical failure of the wrinkle structure. Another test involving mechanical scratching demonstrates that the present system has improved tribological

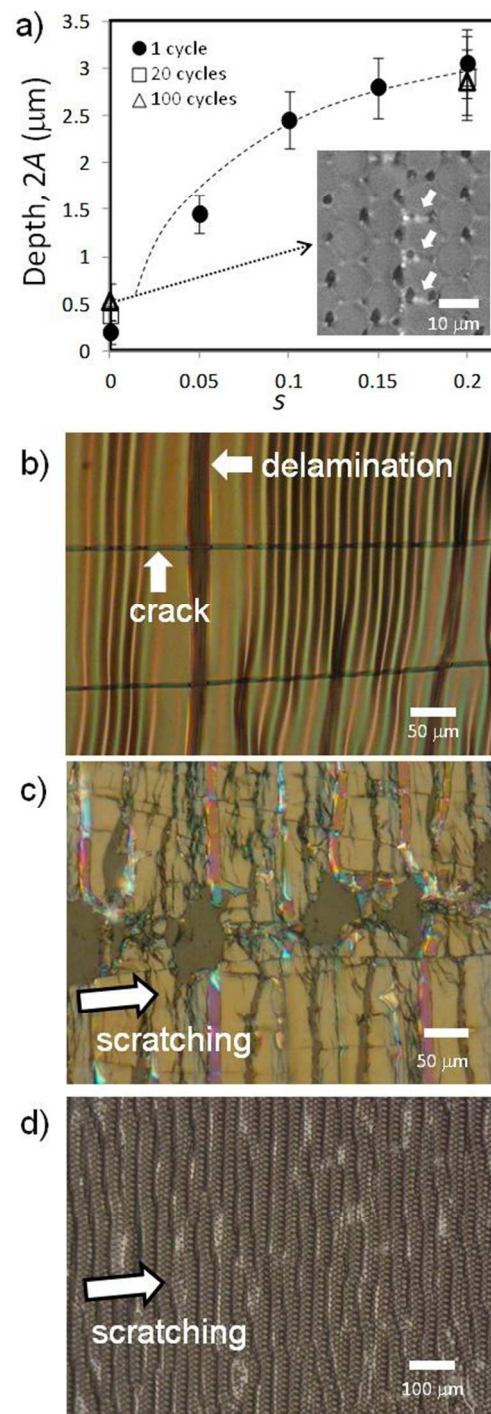


Fig. 3. Mechanical durability. (a) Repeatable shape-(depth)-tunability of wrinkles formed on porous-film-embedded PDMS. (Inset) An optical microscopy image at $s = 0$ after 100 compression–decompression cycles for between $s = 0$ and $s = 0.2$. The positions indicated by white arrows correspond to the beams of the porous structure, at which a crest was located, and appear brighter than those of other beams. These parts are assumed to be slightly delaminated from PDMS inside the sample because of the repeated application of high strain. (b) PSt/PDMS under a strain of $s = 0.15$ shows wrinkles as well as delaminated crests and cracks, indicating low durability against high compressive strain. (c) PS/PDMS under a strain of $s = 0.15$ after a scratching test and showing critical failures. (d) Porous-film-embedded PDMS under a strain of $s = 0.15$ after a scratching test and showing original wrinkles without mechanical failure. (See also SI-Movie S1.)

durability (Fig. 3c, 3d, and SI Movie 1). The PSt/PDMS system is easily destroyed by the present scratching condition. In contrast, the porous-film-embedded surface shows neither scars nor cracks after scratching. The observed mechanical durability is due to the interpenetrated structure between the gauche framework of the porous film and the PDMS matrix; this structure reinforces the effective hard layer for wrinkling and enlarges the material interfacial area, thereby preventing fatal delamination.

Especially, the crack-resistant property on wrinkling, which is a major merit of using the present system, can be attributed to the textile-net-like flexibility of the porous film. The hexagons elongated in the y direction upon wrinkling (Fig. 2b) suggests that the tensile strain in the direction perpendicular to that of compression may be accommodated by rotating the beams with respect to the z axis. As a result, the actual tensile stress applied along the beams should be smaller than that found in the plane film under an identical external strain (or a scratching condition), improving crack-resistance. This mechanical property is similar to that of the textile-net. Moreover, even if some beams crack, the cracked parts are difficult to propagate because of discreteness of the porous structure, preventing critical failure of the wrinkled structure.

In summary, the results obtained in this study demonstrate that a porous polymer film embedded near the surface of a soft elastic substrate self-organizes into microwrinkles, as determined by the applied compressive strain. Although the local structures of the wrinkled surface are coupled to the porous film lattice, the wrinkles show a characteristic wavelength and their depth can be tuned by the degree of strain, which is similar to that in a system of a flat film simply supported by a soft substrate. It is also shown that the bending rigidity of the porous film subjected to wrinkling is increased owing to the gauche architecture. It is of primary importance that the present shape-tunable microwrinkles show improved mechanical durability against mechanical scratching and repeated compression–decompression cycles over a wide strain range (0–0.2). The critical failure for wrinkling is ingeniously suppressed by the present structural design. Most of the relatively fragile porous film is embedded in a soft elastic substrate that mechanically supports the film against deformation and prevents it from coming in direct contact with other bodies. Thus, the mechanical strength of the present surface is comparable to that of the pure elastic material used as the substrate, which typically shows Young's modulus less than tens of megapascals and thus bears high strains by elastic yielding. Moreover, owing to the increased and curvilinear area of the interface between the porous film and PDMS, fatal delamination at the interface, which occurs upon wrinkling, is suppressed. The crack formation is also suppressed owing to the textile-net-like flexibility of the porous film. The characteristic wavelength of the present reinforced microwrinkles can be controlled by varying the bending rigidity of the effective hard layer; the bending rigidity can be altered by changing Young's modulus and the detailed structure of the porous film. The strain-direction-dependent coupling effect of the imprinted lattice structure on the local wrinkle shape may also be reduced or enhanced by appropriate structural designs for the porous film to be embedded; however, this topic remains to be studied further. Thus, the new design presented herein for producing reinforced shape-tunable microwrinkles

provides a promising route to widen the application spectrum of such microwrinkles, which includes tribological applications and switching elements subjected to repeated structural changes.

This work was partially supported by the Japanese Ministry of Education, Culture, Sports, Science and Technology (MEXT) via Grants-in-Aid for Scientific Research on Innovative Areas (Grant No. 24120003 and No. 24120004).

Notes and references

^a Nanosystem Research Institute, AIST, 1-1-1 Higashi, Tsukuba, 305-8565, Japan. E-mail: ohzono-takuya@aist.go.jp.

^b Department of Bio-and Material Photonics, Chitose Institute of Science and Technology, Chitose 066-8655, Japan.

^c Department of Physics, Tohoku University, 6-3 Aramaki Aoba, Sendai, 980-8578, Japan.

Electronic Supplementary Information (ESI) available: Supplementary Information (SI) 1-3, SI Figures S1-S2 and SI Movie 1. See DOI: 10.1039/c000000x/

- H. G. Allen, *Analysis and Design of Structural Sandwich Panels*, Pergamon, New York, **1969**; J. Genzer and J. Groenewold, *Soft Matter* **2006**, *2*, 310; R. Huang, and Z. Suo, *J. Appl. Phys.* **2002**, *91*, 1135; N. Bowden, S. Brittain, A. G. Evans, J. W. Hutchinson and G. M. Whitesides, *Nature* **1998**, *393*, 146; F. Brau, H. Vandeparre, A. Sabbah, C. Poulard, A. Boudaoud and P. Damman, *Nat. Phys.* **2011**, *7*, 56; F. Brau, P. Damman, H. Diamant and T. A. Witten, *Soft Matter* **2013**, *9*, 8177; N. Uchida and T. Ohzono, *Soft Matter* **2010**, *6*, 5792.
- P. J. Yoo and H. H. Lee, *Phys. Rev. Lett.* **2003**, *91*, 154502; T. Okayasu, H. -L. Zhang, D. G. Bucknall and G. A. D. Briggs, *Adv. Funct. Mater.* **2004**, *14*, 1081.
- N. Bowden, W. T. S. Huck, K. E. Paul and G. M. Whitesides, *Appl. Phys. Lett.* **1999**, *75*, 2557.
- T. Ohzono, K. Suzuki, T. Yamaguchi and N. Fukuda, *Adv. Opt. Mater.* **2013**, *1*, 374.
- P. Kim, Y. Hu, J. Alvarenga, M. Kolle, Z. Suo and J. Aizenberg, *Adv. Opt. Mater.* **2013**, *1*, 381.
- K. Efimenko, M. Rackaitis, E. Manias, A. Vaziri, L. Mahadevan and J. Genzer, *Nat. Mater.* **2005**, *4*, 293.
- C. Lu, H. Möhwald and A. Fery, *Soft Matter* **2007**, *3*, 1530.
- T. Ohzono, H. Monobe, N. Fukuda, M. Fujiwara and Y. Shimizu, *Small* **2011**, *7*, 506.
- T. Ohzono and J. Fukuda, *Nat. Commun.* **2012**, *3*, 701.
- X. Jiang, S. Takayama, X. Qian, E. Ostuni, H. Wu, N. Bowden, P. LeDuc, D. E. Ingber and G. M. Whitesides, *Langmuir* **2002**, *18*, 3273.
- C. M. Stafford, C. Harrison, K. L. Beers, A. Karim, E. J. Amis, M. R. Vanlandingham, H. C. Kim, W. Volksen, R. D. Miller and E. E. Simonyi, *Nat. Mater.* **2004**, *3*, 545.
- A. J. Nolte, M. F. Rubner and R. E. Cohen, *Macromolecules* **2005**, *38*, 5367.
- R. Vendamme, T. Ohzono, A. Nakao, M. Shimomura and T. Kunitake, *Langmuir* **2007**, *23*, 2792.
- J. A. Rogers, *ACS Nano* **2007**, *1*, 151.
- W. H. Koo, S. M. Jeong, F. Araoka, K. Ishikawa, S. Nishimura, T. Toyooka and H. Takezoe, *Nat. Photon.* **2010**, *4*, 222.
- J. Y. Chung, J. P. Youngblood and C. M. Stafford, *Soft Matter* **2007**, *3*, 1163.
- K. Khare, J. Zhou and S. Yang, *Langmuir* **2009**, *25*, 12794; T. Ohzono, H. Monobe, K. Shiokawa, M. Fujiwara and Y. Shimizu, *Soft Matter* **2009**, *5*, 4658; H. Monobe, T. Ohzono, H. Akiyama, K. Sumaru and Y. Shimizu, *ACS Appl. Mater. Interface* **2012**, *4*, 2212.
- T. Ohzono, T. Yamamoto and J. Fukuda, *Nat. Commun.* **2014**, *5*, 3735.
- E. P. Chan, E. J. Smith, R. C. Hayward and A. J. Crosby, *Adv. Mater.* **2008**, *20*, 711.
- T. Ohzono and M. Shimomura, *Phys. Rev. B* **2004**, *69*, 132202; T. Ohzono and H. Monobe, *J. Colloid. Interface Sci.* **2012**, *369*, 1.
- S. Yang, K. Khare and P.-C. Lin, *Adv. Funct. Mater.* **2010**, *20*, 2550; C. Cao, H. F. Chan, J. Zang, K. W. Leong and X. Zhao, *Adv. Funct. Mater.* **2014**, *26*, 1763.

- 22 H. Mei, R. Huang, J. Y. Chung, C. M. Stafford and H.-H. Yu, *Appl. Phys. Lett.* 2007, **90**, 151902.
- 23 C. J. Rand and, A. J. Crosby, *J. Appl. Phys.* 2009, **106**, 064913; L. Skedung, M. Arvidsson, J.Y. Chung, C. M. Stafford, B. Berglund and M. W. Rutland, *Sci. Rep.* 2013, **3**, 2617.
- 24 H. Yabu, Y. Hirai and M. Shimomura, *Langmuir* 2006, **22**, 9760; Y. Hirai, H. Yabu, Y. Matsuo, K. Ijiro and M. Shimomura, *J. Mater. Chem.* 2010, **20**, 10804.
- 25 G. Widawski, M. Rawiso and B. Francois, *Nature* 1994, **369** 387; T. Nishikawa, R. Ookura, I. Nishida, K. Arai, I. Hayashi, N. Kurono, T. Sawadaishi, M. Hara and M. Shimomura, *Langmuir* 2002, **18**, 5734.
- 26 The value of H (and the wrinkle wavelength) should vary nonlinearly with the detailed structural parameters of the porous film, e.g., shapes of beams and pillars, periodicity, etc.. Although in the present specific experimental conditions the wrinkle wavelength results in 3-4 times that of the pore periodicity, the general relationship between H and the complicated structural parameters is unknown and remains to be clarified experimentally and theoretically. Thus, the present result should not be a general one. Nevertheless, it is noted that similar geometrical relationship is found when we use a smaller periodicity, $\lambda \sim 7 \mu\text{m}$, for the porous film composed of the same material [see Fig. S2d].
- 27 D. Qian, E. C. Dickey, R. Andrews and T. Rantell, *Appl. Phys. Lett.* 2000, **76**, 2868.
- 28 T. Ohzono, H. Watanabe, R. Vendamme, C. Kamaga, T. Ishihara, T. Kunitake and M. Shimomura, *Adv. Mater.* 2007, **19**, 3229; T. Ohzono, S. I. Matsushita and M. Shimomura, *Soft Matter* 2005, **1**, 227; T. Ohzono, *Chaos* 2009, **19**, 033104; C. F. Guo, V. Nayyar, Z. Zhang, Y. Chen, J. Miao, R. Huang and Q. Liu, *Adv. Mater.* 2012, **24**, 3010; C.-M. Chen, J. C. Reed and S. Yang, *Soft Matter* 2013, **9**, 11007.